Journal of Catalysis
doi:10.1006/jcat.2001.3453, available online at http://www.idealibrary.com on IDEAL®

Low-Temperature Hydrodesulfurization of Thiophene on Ni/Pt(111) Bimetallic Surfaces with Monolayer Ni Coverage

Neetha A. Khan, Henry H. Hwu, and Jingguang G. Chen[1]

Center for Catalytic Science and Technology (CCST), Department of Materials Science and Engineering, University of Delaware, Newark, Delaware 19716

Received May 17, 2001; revised September 24, 2001; accepted September 24, 2001

The low-temperature HDS of thiophene was investigated over Ni/Pt(111) bimetallic surfaces using Auger electron spectroscopy, temperature-programmed desorption, and low-energy electron diffraction. The reactivity of the bimetallic surface, with Ni coverages at approximately one monolayer (ML), was compared to those of a Pt(111) surface and thick Ni(111) film. All surfaces decomposed thiophene; however, Ni/Pt(111) and thick Ni(111) produced butene. More importantly, the desorption of butene from the monolayer Ni/Pt(111) surface occurred at a significantly lower temperature (∼230 K) than that of the Ni(111) film (∼280 K). In addition, the Ni/Pt(111) and Pt(111) surfaces also produced butadiene. The selectivity to produce C_4 hydrocarbon molecules on the Ni/Pt(111) surface remained similar to that of the Pt(111) surface. However, the overall activity toward the decomposition of thiophene increased from 0.053 thiophene per metal atom on Pt(111) to 0.077 thiophene per metal atom on the monolayer Ni/Pt(111) surface. The preadsorption of atomic hydrogen at liquid nitrogen temperatures on the ML bimetallic Ni/Pt surface further enhanced the activity toward the production of gas-phase butene by a factor of 2.2. We propose that this increase in the HDS activity on the monolayer Ni/Pt(111) surface results from the weak M–H bond, not seen on either pure metal surface.

Key Words: **thiophene; HDS; monolayer Ni; Pt(111); Ni(111).**

1. INTRODUCTION

Thiophene, C_4H_4S, is often used as a model molecule for surface science investigations of the hydrodesulfurization (HDS) process (1–3). HDS is an industrially critical process because it extracts sulfur from hydrocarbon feed streams such as crude oil, coal, and petroleum. If left untreated, the sulfur in the feed proceeds to rapidly poison catalysts used in subsequent reforming processes. In addition, minimizing the sulfur content in gasoline and diesel fuels prevents the formation of sulfur oxides, which are environmentally hazardous compounds. Finally, sulfur has also been identified as a poison for automotive catalytic converters (1). It is therefore significant to identify efficient HDS catalysts and to fundamentally understand the nature of the C–S bond cleavage.

The HDS mechanisms of thiophene have been extensively investigated and are generally well understood. From a variety of kinetic studies it is concluded that the HDS of thiophene can occur *via* two mechanisms: (i) hydrogenation, where the C_4H_4S ring is hydrogenated before HDS; or (ii) hydrogenolysis, where the cleavage of the C–S bonds occurs without first saturating the C_4H_4S ring (4). In addition, the decomposition mechanisms of thiophene and methyl-substituted thiophenes have been the subject of several detailed surface science studies (5–8). In these studies, various surface techniques were applied to determine the identity and bonding orientation of chemisorbed thiophenes and the HDS intermediates on well-ordered single crystal surfaces; the conclusions from these studies provided additional insights into the overall understanding of the HDS mechanisms of thiophene molecules (6–8).

As typically observed for the HDS of many organosulfur compounds (9), the HDS of thiophene is an exothermic reaction, for example,

$$C_4H_4S + 3H_2 \rightarrow C_4H_8 + H_2S \quad [1]$$

$$C_4H_4S + 2H_2 \rightarrow C_4H_6 + H_2S. \quad [2]$$

Using thermodynamic values for both reactions (10, 11), the free energy of the two reactions at 298 K was determined to be −88.6 and −9.9 kJ/mol, respectively. As shown in Fig. 1, the free energy for the HDS of thiophene was negative at low temperatures (∼475 K) and positive at higher temperatures (at $T > 475$ K for the formation of 1,3-butadiene and at $T > 850$ K for butene). Therefore, the HDS reaction would be favored at low temperatures but increasingly unfavorable at higher temperatures. However, the HDS of thiophene is kinetically limited, as suggested by a relatively small rate constant (1.38×10^{-3} L/g of catalyst · s) at 573 K. As a result, the industrial conditions for this reaction are consequently at high temperature (533–623 K) and high H_2 pressure to overcome this kinetic barrier (9).

It is well known from literature that the chemical properties of bimetallic systems are often different from those of

[1] To whom correspondence should be addressed. Fax: 302-831-4545. E-mail: jgchen@udel.edu.

0021-9517/02 $35.00

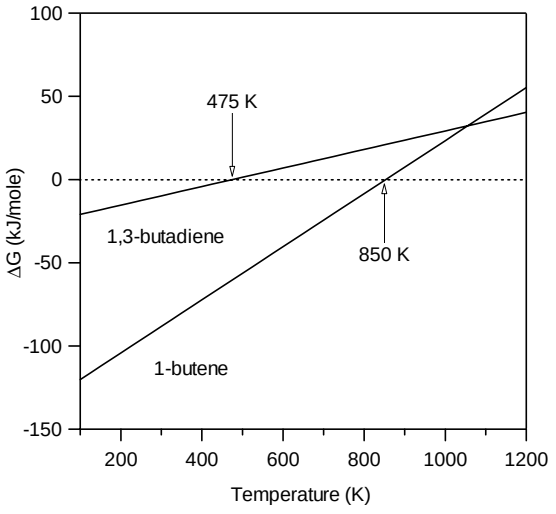

FIG. 1. A plot of free energy of the gas-phase HDS reaction of thiophene as a function of temperature.

either parent metals (12–16). For example, Goodman and co-workers observed that Ni/Pt surfaces with near monolayer (ML) Ni coverages on Pt showed higher hydrogenolysis activity than pure Ni or Pt surfaces (16). In our prior work, we have identified several novel chemical reactions on Ni/Pt surfaces which are characterized by a Ni coverage at approximately one monolayer (12, 17). Briefly, recombinative D_2 desorption occurred at a lower temperature for bimetallic Ni/Pt(111) than for either Ni(111) or Pt(111). We have also found that the hydrogenation of cyclohexene occurred under ultrahigh vacuum (UHV) conditions on the bimetallic surface but not on either pure metal surface (17). For this study, we attempt to determine whether the weak metal–hydrogen bonds would lead to the low-temperature HDS of thiophene over Ni/Pt bimetallic surfaces. We will concentrate on the comparison of HDS chemistry over monolayer Ni/Pt(111), Pt(111), and thick Ni(111) films.

2. EXPERIMENTAL

The UHV chamber used in these studies is a two-level stainless-steel chamber (base pressure of 2×10^{-10} Torr) equipped with Auger electron spectroscopy (AES), low-energy electron diffraction (LEED), and temperature-programmed desorption (TPD). For TPD experiments, the Pt(111) sample was heated with a linear heating rate of 3 K/s. In addition, the opening of the random flux shield of the quadrupole mass spectrometer was placed at a distance of ~5 mm from the sample surface. The experimental setup allowed us to monitor up to 12 masses simultaneously.

The single crystal sample was a [111] oriented 1.5-mm-thick platinum disk (99.999%), 12 mm in diameter, purchased from Metal Crystals and Oxides, Ltd., Cambridge, England. The crystal was spot-welded directly to two tantalum posts that serve not only as electrical connections for resistive heating but also as thermal contacts for cooling with liquid nitrogen. With this mounting scheme, the temperature of the crystal could be varied between 90 and 1300 K. Thiophene (Aldrich, 99+% purity) was purified by successive freeze–pump–thaw cycles prior to their use. The purity was verified *in situ* by mass spectrometry. Oxygen, neon, hydrogen, and deuterium were all of research grade purity and were introduced into the UHV chamber without further purification. Doses are reported in langmuirs ($1\ \text{Langmuir} = 1 \times 10^{-6}$ Torr · s) and are uncorrected for ion gauge sensitivities. In all experiments, thiophene exposures were made at a crystal temperature of 120 K with the crystal surface located in front of a 10-mm-diameter directional dosing tube.

A clean Pt(111) crystal surface is prepared by cycles of Ne^+ bombardment at 400 K (sample current ~8 μA) and flashing to 1100 K. These 7-min cycles are generally repeated three times before annealing at 1100 K for ~5 min. AES analysis shows that the C and O impurities are both less than 1% of a monolayer after the previous cleaning procedure. LEED was then used to confirm the order of the Pt(111) surface. Nickel was deposited from an evaporative doser, which consisted of a resistively heated tungsten filament, tightly wrapped with ultrapure Ni wire (99.999% Ni, 0.25 mm in diameter), mounted on a stainless-steel enclosure with a 1-cm-diameter opening. After initial conditioning, the amount of impurity buildup was below the detection limit of AES. During deposition, the Pt(111) crystal was positioned approximately 2 cm from the Ni doser opening, with the surface perpendicular to the doser axis.

The preparation of the Ni/Pt(111) bimetallic surfaces was described in detail previously (12). Briefly, the substrate was maintained at 600 K during deposition, and the Ni deposition remained uniform across the substrate surface. The coverage of the Ni overlayer was estimated based on the reduction of the Pt(237 eV) peak after the deposition of Ni (12). Thick Ni films were generated by exposure to Ni until the Pt Auger signal was within the noise level. LEED measurements revealed a sharp (111) pattern, confirming the epitaxial growth of Ni on Pt(111) at 600 K.

3. RESULTS AND DISCUSSION

3.1. Adsorption of D_2 over Pt(111), One ML Ni/Pt(111), and Thick Ni(111) Film

Figure 2 shows D_2 desorption spectra after exposing the three surfaces to saturation exposures (50 L) at 120 K. Recombinative D_2 desorption occurs at ~287 and ~322 K for Pt(111) and thick Ni(111) film, respectively. The thick Ni(111) film is representative of the Ni(111) crystal surface, as shown by the similar peak shape and desorption temperature in the top two spectra. In contrast, the recombinative D_2 desorption temperature on ML Ni/Pt(111) is lower than

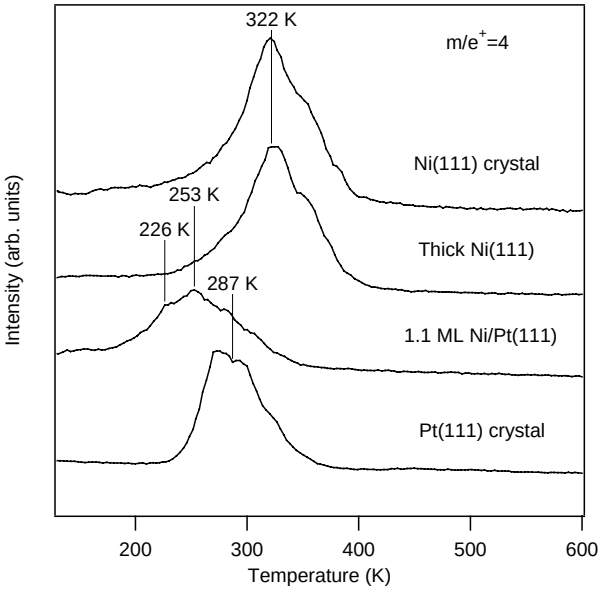

FIG. 2. TPD spectra of a saturation exposure of 50 L D_2 on Pt(111), Ni/Pt(111), and Ni(111) surfaces.

that on either parent metal. The desorption peak of D_2 is centered at 253 K, with a low temperature shoulder at 226 K. These results are consistent with prior experimental studies on 50% Pt–50% Ni bulk alloys and theoretical studies of Pt monolayers on Ni(111), which showed reduced chemisorption strength for atomic hydrogen when compared to that for pure components (18).

In principle, the reaction pathways of HDS on Pt(111), Ni/Pt(111), or thick Ni(111) surfaces should be dependent on the metal–hydrogen bond strength of surface hydrogen.

As stated earlier, the HDS of thiophene involves both the cleavage of the C–S bond of thiophene and the cleavage of the metal–hydrogen bond to produce C_4 products. The D_2 experiments in Fig. 2 clearly indicate that hydrogen atoms are more weakly bonded to the Ni/Pt(111) bimetallic surface and may therefore lead to an increase in the activity of the bimetallic surface toward the HDS of thiophene.

3.2. Decomposition of Thiophene over Pt(111), Ni/Pt(111), and Thick Ni(111) Film

3.2.1. TPD results. Figures 3 and 4 show TPD results after exposing Pt(111), Ni(111) thick film, and monolayer Ni/Pt(111) surfaces to 0.5 L of thiophene at 120 K. Because of the utilization of the directional dosing tube, an exposure of 0.5 L corresponds to a multilayer coverage, as indicated by the presence of a multilayer desorption peak at 152 K. All TPD experiments of thiophene were performed by exposing surfaces to this coverage. The major desorption products detected were molecular thiophene (84 amu), H_2 (2 amu), butene (41 amu), and a small amount of butadiene (39 amu). The TPD of mass 84 shows only two peaks, a large multilayer peak at 152 K and a smaller monolayer peak at ~170 K. The monolayer peak for the Ni/Pt(111) surface is slightly lower in temperature than that for either pure metal surface. The detection of mass 2 amu at higher temperatures indicates that some of the thiophene decomposes to produce gas-phase hydrogen and surface carbon and sulfur. (The latter two are confirmed by Auger measurements.) All three surfaces are active toward thiophene decomposition, as evident by the presence of broad peaks in the H_2 TPD spectra. Figure 3 also shows that H_2 desorbs from all three surfaces through a series of overlapping peaks, ranging from

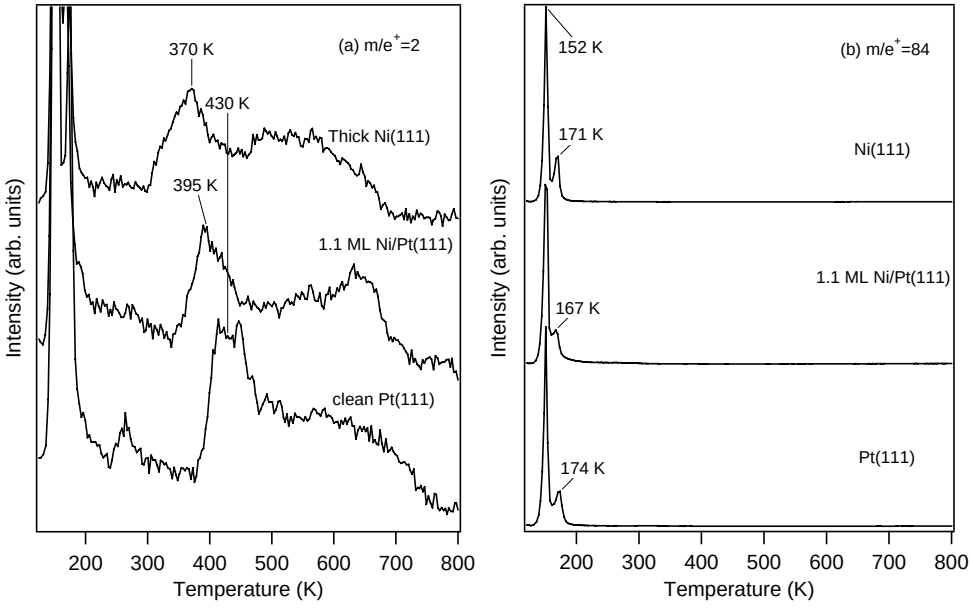

FIG. 3. TPD spectra of hydrogen gas (a) and molecular thiophene (b) from the reaction of 0.5 L thiophene on different surfaces.

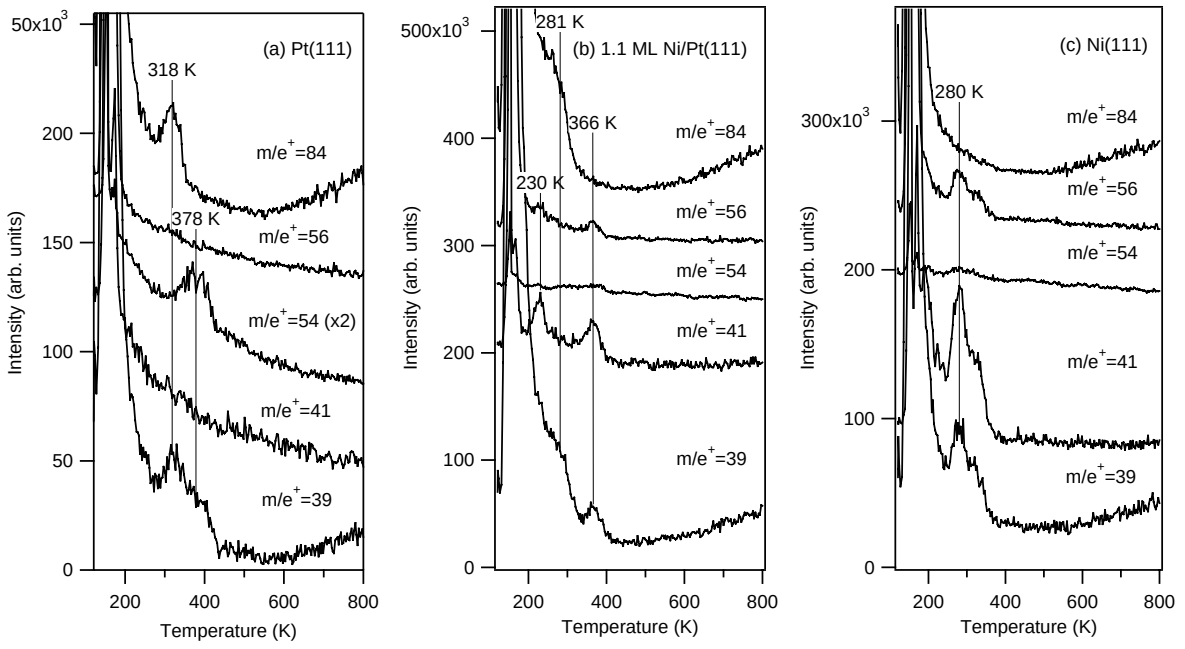

FIG. 4. A comparison of TPD spectra of C_4 hydrocarbon products and the thiophene molecular spectra ($m/e^+ = 84$) from the reaction of 0.5 L thiophene on different surfaces.

350 to 700 K. However, the temperature of the first peak on Ni/Pt(111) and thick Ni(111) surfaces is lower than that on Pt(111). The H_2 spectra on the pure metal surfaces are consistent with those of literature data from the decomposition of thiophene on Ni(111) and Pt(111)(6, 19).

The production of butene is present only on Ni/Pt(111) and thick Ni(111), as shown in Fig. 4. Butene desorbs from the Ni/Pt(111) bimetallic surface at two temperatures—230 and 366 K. However, on the thick Ni(111) film, butene does not start desorbing from the surface until about 280 K. The overall areas for both peaks indicate that about the same amount of butene is produced on both surfaces. It may seem that butadiene is also produced on Ni(111), but the similar peak shape and desorption temperature indicate that the $m/e^+ = 39$ peak is due to the cracking pattern of butene. The peak area ratio between mass 39 amu and mass 41 amu is approximately 0.6 on Ni(111), which corresponds to the ratio in the cracking pattern of butene in our control experiments.

A small amount of butadiene desorbs from the Pt(111) surface at 364 K, which is consistent with previous results of reaction of thiophene on Pt(111) (1). The peak for $m/e^+ = 39$ on Pt(111) is actually a combination of two peaks (cracking pattern from strongly chemisorbed molecular thiophene at 318 K and butadiene at 378 K), as compared in the left panel in Fig. 4. In order to accurately calculate the amount of butadiene being produced on Pt(111), the peak from the thiophene cracking pattern was subtracted from that of butadiene, in accordance with the cracking pattern ratio. Therefore, the butadiene production is less than the TPD spectrum indicates. Butadiene is also produced on the Ni/Pt(111) surface at 366 K. The shoulder peak at ~280 K for $m/e^+ = 39$ on Ni/Pt(111) is due to the cracking pattern of thiophene. For ease of comparison, TPD spectra of the parent molecules of butadiene (54 amu) and butene (56 amu) are also included in Fig. 4. While only the TPD spectra of butadiene and butene are shown, we also monitored propylene, ethylene, methane, butane, and H_2S in the TPD experiments; these products were not observed in our measurements.

Furthermore, the comparison of the relative intensities of masses 56 and 41 amu in the TPD spectra in Fig. 4 also suggests that different butene isomers are produced on Ni/Pt(111) and thick Ni(111) film. On the thick Ni(111) film, the intensity ratio of 56 amu/41 amu is approximately 0.33, which is expected for the cracking pattern of 1-butene (10). On the other hand, the ratio is approximately 0.48 on the monolayer Ni/Pt(111) surface, which is indicative of 2-butene (10). However, more detailed spectroscopy studies are needed in subsequent experiments to understand the origin of the different butene products of the HDS reaction of thiophene on the two surfaces.

3.2.2. Product selectivity. Based on the obtained TPD results, it is clear that a fraction of thiophene undergoes complete decomposition on all three surfaces. The complete decomposition can be expressed as

$$C_4H_4S(\text{ads}) \rightarrow 4C(\text{ads}) + 2H_2(g) + S(\text{ads}) \qquad [3]$$

a	$4a$	$2a$	a	on Pt(111)
c	$4c$	$2c$	c	on Ni/Pt(111)
f	$4f$	$2f$	f	on Ni(111).

The reaction to produce butene, seen on Ni/Pt(111) and the Ni(111) film, can be expressed as

$$C_4H_4S(ads) + 4H(ads) \rightarrow C_4H_8(g) + S(ads) \quad [4]$$

g $2g$ g g on Ni(111)

d $2d$ d d on Ni/Pt(111).

Finally, the reaction to produce butadiene, seen on both Pt(111) and Ni/Pt(111), can be expressed as

$$C_4H_4S(ads) + 2H(ads) \rightarrow C_4H_6(g) + S(ads) \quad [5]$$

b b b b on Pt(111)

e e e e on Ni/Pt(111).

From the AES measurements of the C (272 eV)/Pt (237 eV) and S (150 eV)/Pt (237 eV) ratios after the TPD experiments on Pt(111), the values for a and b were estimated to be 0.031 and 0.022, respectively. These atomic ratios were calculated using the standard sensitivity factors for C, S, and Pt (20). The ratio of the TPD peak areas of butadiene between Pt(111) and Ni/Pt(111), after subtracting the contributions from the cracking patterns of thiophene and butene, respectively, was calculated to be 2.65. This leads to the following relationship:

$$\frac{C_4H_6 \text{ on Pt}}{C_4H_6 \text{ on Ni/Pt}} = 2.65 = \frac{b}{e}. \quad [6]$$

In order to calculate the amount of butene produced on Ni/Pt(111) (d value), the mass spectrometer sensitivity was checked by dosing butadiene and butene separately into the chamber at the same pressure. The peak ratio of the mass 39 from butadiene and mass 41 from butene was found to be 0.75. Therefore, the peak areas of butene were multiplied by 0.75 to correct for the different sensitivity factors for the mass spectrometry measurements. This leads to the following relationship:

$$\frac{C_4H_6 \text{ on Ni/Pt}}{C_4H_8 \text{ on Ni/Pt}} = 0.19 = \frac{e}{d}. \quad [7]$$

The value, 0.19, corresponds to the ratio of the peak areas of butadiene to butene on the Ni/Pt(111) surface, after normalizing the area of butene by the relative sensitivity factor of 0.75. Based on the results shown in Fig. 2, we calculated the ratio of the peak areas of hydrogen desorption between Pt(111) and Ni/Pt(111) to be 1.23. This leads to

$$\frac{H_2 \text{ on Pt}}{H_2 \text{ on Ni/Pt}} = 1.23 = \frac{2a - b}{2c - 2d - e}. \quad [8]$$

From Eqs. [6]–[8], the values for c, d, and e were calculated to be 0.045, 0.027, and 0.005, respectively. In order to quantify the butene formation on the thick Ni(111) film, the following relationships were used:

$$\frac{H_2 \text{ on Ni}}{H_2 \text{ on Pt}} = 0.77 = \frac{2f - 2g}{2a - b} \quad [9]$$

TABLE 1

Selectivity for the Three Surfaces toward the Production of C_4 Hydrocarbons

Surface	Selectivity (%)		Activity (C_4H_4S/Pt)		T_p (K) C_4H_6 (or C_4H_8)
	C_4	Decomposition	C_4	Decomposition	
Pt(111)	41.5	58.5	0.022	0.031	364
Ni/Pt(111)	41.6	58.4	0.032	0.045	230
Ni(111)	41	59	0.034	0.049	280
H/Ni/Pt(111)	—	—	0.071	—	246

$$\frac{C_4H_8 \text{ on Ni}}{C_4H_8 \text{ on Ni/Pt}} = 1.30 = \frac{g}{d}. \quad [10]$$

The values for f and g were calculated to be 0.049 and 0.034, respectively. From the values for a–g, the selectivities and activities of the three surfaces were calculated, as shown in Table 1. The selectivity of the three surfaces seems to be similar. However, the overall activities, defined as the number of decomposed thiophene on a per Pt atom basis, are larger for the Ni/Pt(111) surface and the Ni(111) film than that for Pt(111).

It should be pointed out that the AES Ni/Pt ratio decreases after the TPD experiments at 800 K. For the monolayer Ni surface, the AES Ni/Pt ratio decreases from ~1.0 to 0.64. Such a decrease can be attributed to either the agglomeration of Ni on the Pt(111) surface or the diffusion of Ni into the Pt(111) substrate. More structural sensitive tools such as scanning tunneling microscopy (STM) and ion scattering spectroscopy (ISS) will be utilized to further characterize the thermal stability of the Ni/Pt(111) overlayer.

3.3. Decomposition of Thiophene on Surfaces with Preadsorbed $H_{(a)}$ and $D_{(a)}$

Figures 5 and 6 compare the effect of preadsorption of 0.5 L hydrogen on the HDS activity of the three surfaces. From the comparison of H_2 TPD as a function of H_2 exposure on Ni/Pt(111) (spectra not shown), the TPD peak area of 0.5 L H_2 is about 37% of that after the saturation exposure (50 L). The TPD spectra in Fig. 5 indicate that preadsorbed hydrogen substantially affects the amount of butene produced from the HDS of thiophene on the Ni/Pt(111) bimetallic surface. The low-temperature peak of the mass 41 amu TPD spectra significantly increases when 0.5 L of H_2 is preadsorbed with 0.5 L of thiophene. In addition, a more pronounced low-temperature mass 39 amu peak is observed at 246 K from the Ni/Pt(111) surface when hydrogen is preadsorbed on the surface.

In contrast, the preadsorption of hydrogen has little or no effect on the HDS activity on either Pt(111) or thick Ni(111)

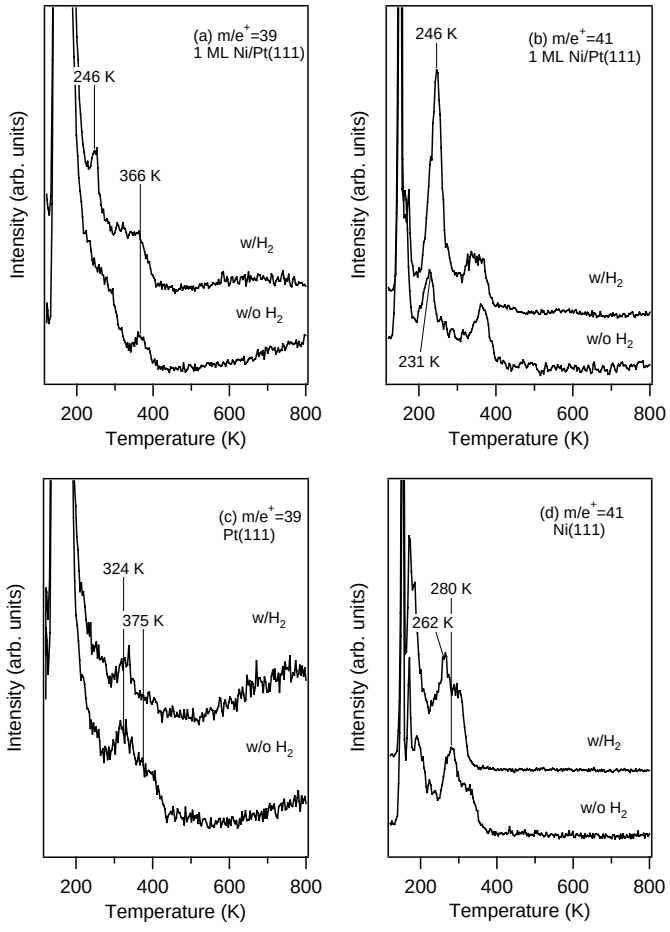

FIG. 5. Butene and butadiene desorption spectra from the reaction of 0.5 L thiophene with and without preadsorbed H_2.

film. The peak area of butadiene on Pt(111) is slightly reduced after the preadsorption of hydrogen, most likely due to the siteblocking by preadsorbed hydrogen. The preadsorption of H on the Ni(111) film causes a slight decrease in the desorption temperature of butene, from 280 to 262 K. However, the peak areas of butene are not noticeably affected by the preadsorption of hydrogen.

When D_2 is preadsorbed onto the surfaces, mass 43 appears in the spectra on the monolayer Ni/Pt(111) surface in which the temperature of deuterated butene ($m/e^+ = 43$) lies at the same temperature as the butene desorption temperature (246 K), as shown in Fig. 6a. To confirm that mass 43 amu is from the preadsorption of D_2, a TPD spectrum of mass 43 amu from thiophene adsorbed on the surface without D_2 is also compared in Fig. 6, which does not show any desorption peaks. Figure 6a also shows that the production of deteruated butene occurs even after exposing the Ni/Pt(111) bimetallic surface to a saturation exposure of 50 L D_2. A slightly smaller amount is seen likely resulting from the competition for sites between thiophene and hydrogen. There is no high-temperature peak for mass 43 observed at ~366 K in Fig. 6a, indicating that all the preadsorbed D_2 is either incorporated into butene or desorbed from the surface by 366 K. As shown in Fig. 6b, the atomic D can be incorporated into the deuterated butene product in several ways. Both deuterated butene products will lose the end methyl group in the mass spectrometer, leading to the detection of mass 43 amu. A peak at 246 K is detected at both $m/e^+ = 60$ and 59, clearly indicating the incorporation of D into the butene products.

From the TPD spectra shown in Figs. 5 and 6, it is clear that preadsorbed hydrogen significantly increases the production of C_4 hydrocarbons for the HDS of the thiophene on Ni/Pt(111). For example, the overall peak area of butene in Fig. 5b on Ni/Pt(111) is increased by a factor of 2.2 as a result of the preadsorbed hydrogen. More quantitatively, this increase indicates that the activity for the production of butene is enhanced from 0.032 to 0.070 thiophene molecules per Pt atom.

It is important to stress the influence of the M–H bond strength on the rates of hydrodesulfurization on the

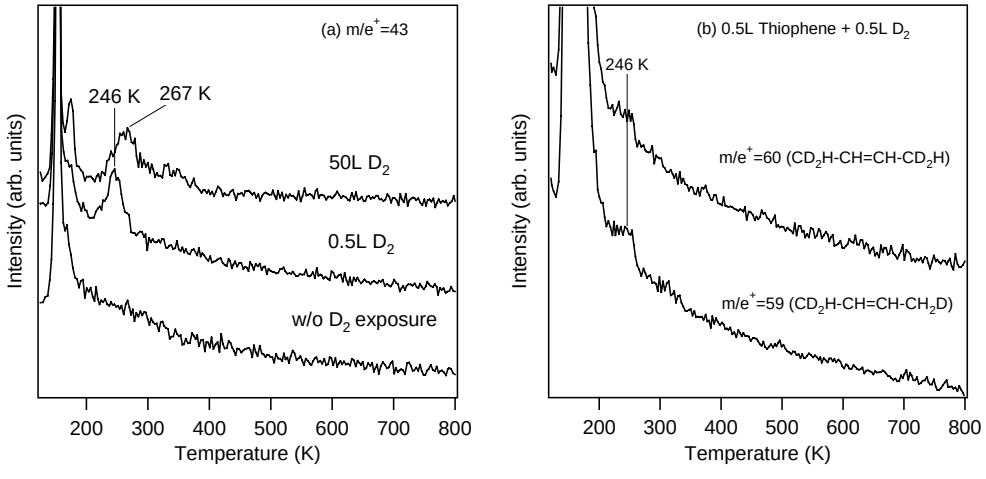

FIG. 6. Possible deuterated butene products desorbing from a ML Ni/Pt(111) bimetallic surface when 0.5 L D_2 is preadsorbed with 0.5 L thiophene.

monolayer Ni/Pt(111). It is evident from the TPD results in Figs. 5 and 6 that hydrogen and deuterium have a promotional effect on the production of butene on the Ni/Pt(111) surface. Only the low-temperature peak (between 230 and 246 K) significantly increases with the addition of hydrogen or deuterium on the surface. This low-temperature peak also corresponds to the temperature at which the M–H (M–D) bonds are cleaved and $H_2(D_2)$ is produced. Furthermore, a similar promotional effect for the production of C_4 is not observed on Pt(111) or thick Ni(111) film, which is most likely due to the stronger M–H bonds on these two surfaces.

Finally, it is useful to compare our results to previous studies of the hydrogenation activity of $Ni_xPt_{1-x}(111)$ alloy surfaces by Massardier and Bertolini. For example, for the hydrogenation of butadiene (21), these authors found that the hydrogenation activity of the $Ni_{0.5}Pt_{0.5}(111)$ surface was higher than that of Pt(111). Because of the segregation of Pt onto the $Ni_xPt_{1-x}(111)$ alloy surfaces (21), it is difficult to directly compare the results from the Pt-covered PtNi(111) alloy surfaces with the current study on monolayer Ni/Pt(111). However, both studies clearly indicate that the presence of Ni enhances the hydrogenation activity of Pt(111).

4. CONCLUSIONS

In this study we have shown that the monolayer Ni/Pt(111) bimetallic surface is active toward the low-temperature HDS of thiophene. All three surfaces decompose thiophene. The bimetallic surface and the thick Ni(111) film are active in the production of butene, while the Pt(111) surface produces a smaller amount of butadiene. However, the bimetallic Ni/Pt(111) surface produces butene at a significantly lower temperature. This low-temperature peak corresponds directly to the weak M–H bond seen on the monolayer Ni/Pt(111) surface. The selectivities of all three surfaces are relatively similar, but the Ni/Pt(111) and Ni(111) film show higher activites for the decomposition and HDS of thiophene.

In addition, the TPD spectra in Figs. 5 and 6 confirm the low-temperature incorporation of $D_{(a)}$ and $H_{(a)}$ into the HDS reaction of thiophene on the Ni/Pt(111) bimetallic surface. The reaction selectivity toward low-temperature butene also can be increased significantly by the preadsorption of hydrogen. Overall, our results indicate that the formation of weaker metal–hydrogen bonds is a potential way to overcome the kinetic barrier for the HDS of thiophene. More studies using XPS and NEXAFS (near edge X-ray absorption fine structure) will be conducted in the near future to further investigate the bonding mechanisms and reaction intermediates on the three surfaces.

ACKNOWLEDGMENTS

We are grateful to thank M. Buelow and M. Zhang for their help in this research. We acknowledge financial support from the Department of Energy (Grant DOE/BES DE-FG02-00ER15104). N. A. Khan and H. H. Hwu also acknowledge financial support from the Presidential Fellowship from the University of Delaware.

REFERENCES

1. Stohr, J., *in* "NEXAFS Spectroscopy," pp. 330–333. Springer-Verlag, New York, 1992.
2. Czogala, C., *Sulfur Rep.* **3**, 12 (1983).
3. Mitchell, P. C. H., *in* "Catalysis" (C. Kemball, Ed.), Vol. 1, p. 223; Vol. 4, p. 203. The Chemical Society, London 1997.
4. Topsoe, H., Clausen, B. S., and Massoth, F. E., "Hydrotreating Catalysis." Springer, New York, 1996.
5. Bent, B. E., *Chem. Rev.* **96**, 1361 (1996).
6. Huntley, D. R., Mullins, D. R., and Wingeier, M. P., *J. Phys. Chem.* **100**, 19,620 (1996).
7. Stohr, J., Gland, J. L., Collin, E. B., Koestner, R. J., Johnson, A. L., Muetterties, E. L., and Sette, F., *Phys. Rev. Lett.* **53**, 2161 (1984).
8. Rodriguez, J. A., Dvorak, J., and Jirsak, T., *Surf. Sci. Lett.* **457**, L413 (2000).
9. Girgis, M. J., and Gates, B. C., *Ind. Eng. Chem. Res.* **30**, 2021 (1991).
10. www.webbook.nist.gov/chemistry.
11. Karapet'yants, M. Kh., and Karapet'yants, M. L., *in* "Thermodynamic Constants of Inorganic and Organic Compounds" (Translation by J. Schmorak), pp. 343–344. Humphrey Science Publishers, Ann Arbor, MI, 1970.
12. Fruhberger, B., Eng, J., Jr., and Chen, J. G., *Catal. Lett.* **45**, 85 (1997).
13. Campbell, C. T., *Annu. Rev. Phys. Chem.* **41**, 775 (1990).
14. Rodriguez, *Surf. Sci. Rep.* **24**, 223 (1996).
15. Xu, C., and Koel, B. E., *Surf. Sci.* **304**, 249 (1994).
16. Goodman, D. W., *Ultramicroscopy* **34**, 9 (1990).
17. Hwu, H. H., Eng, J., Jr., and Chen, J. G., in preparation.
18. Cabeza, G. F., Castellani, N. J., and Légaré, P., *Comp. Mater. Sci.* **17**, 255 (2000).
19. Lang, J. F., and Masel, R. I., *Surf. Sci.* **183**, 44 (1987).
20. Hedberg, C. L., Ed., "Handbook of Auger Electron Spectroscopy," 3rd edition. Physical Electronics, Eden Prairie, MN, 1995.
21. Massardier, J., and Bertolini, J. C., *J. Catal.* **90**, 358 (1984).